

# A SEAT BELT BUCKLE PRETENSIONER AND LOAD-LIMITER COMBO DEVICE

**J. T. Wang**

**Qing Zhou\***

General Motors Corporation

USA

Paper No. 144

\*Currently with Volpe Research

## ABSTRACT

Pretensioners and load-limiters are two well-known safety devices for seat belt systems of motor vehicles. The pretensioner is used to rapidly remove belt slack in the very early stage of a crash event. On the other hand, the load-limiter is used in the later stage of a crash event to regulate the maximum seat belt force acting on the occupant and to control the occupant forward excursion. In this paper, we present a linear pretensioner and load-limiter combo device, which possesses the advantages of both pretensioner and load-limiter but without the corresponding packaging, mass and cost disadvantages. In this two-in-one design, the webbing displacement induced by the operation of a linear pretensioner is reused for load-limiting purposes. A mechanics model is developed to analytically estimate the load-limiting force and to understand relations among system variables and performance. Using this model, the equation of load-limiting force was derived. A prototype device was designed, built and tested to verify the validity of the model. While the linear pretensioner and load-limiter combo device is integrated into the seat belt buckle, it is also suitable to be integrated into the shoulder belt height adjuster due to its linear construction. Since the device is only the size of a buckle pretensioner, it eliminates the packaging, mass and cost associated with an additional load-limiter.

## INTRODUCTION

Pretensioners and load-limiters are two look-alike but very different safety devices for seat belt systems of modern motor vehicles [1]. The pretensioner is used to generate tension forces in the shoulder belt and/or the lap belt immediately after it is activated by a crash sensing system. The tension force will then rapidly remove belt slack in the very early stage of a crash event. On the other hand, the load-limiter is used in the later stage of a crash event to regulate the maximum seat belt force acting on the occupant and to control the occupant forward excursion.

While the use of pretensioners and load-limiters could enhance the crash performance of a seat belt system in some crashes, the use of both devices in a

seat belt system has not always been a practical choice due to the following considerations: (1) The interaction between a pretensioner and a load-limiter must be managed by limiting the pretensioning force to a level less than the load-limiting force; (2) it will double the packaging requirement since the size of a pretensioner is approximately the same as a load-limiter; and (3) it will double the mass and cost since the unit mass and cost of a pretensioner and a load-limiter are approximately the same.

In this paper, we present a linear pretensioner and load-limiter combo device [2], which possesses the advantages of both pretensioner and load-limiter but without the corresponding packaging, mass and cost disadvantages. The linear pretensioner and load-limiter combo device is integrated into the seat belt buckle assembly. In this two-in-one design, the webbing displacement induced by the operation of a linear pretensioner is reused for load-limiting purposes. A mechanics model to analytically estimate the load-limiting force and to understand relations among system variables and performance, is also presented. Using this model, the equation of load-limiting force was derived. A prototype device was designed, built and tested to verify the validity of the model.

## BASIC CONCEPT

Consider a typical linear buckle pretensioner (see Fig. 1). Its basic structural elements include a tube attached to the motor vehicle body through a bracket, a shuttle (also referred to as a piston in literature) inside the tube, a connecting member between the seat belt buckle and the shuttle, a source of high-pressure gas, and a self-locking mechanism.

When sensors on the motor vehicle detect rapid deceleration characteristic of a collision, high-pressure gas is injected into a chamber between the head end of the tube and the shuttle. The gas propels the shuttle through a tension stroke during seat belt webbing, through the connecting member, is pulled, removing slack. At the conclusion of the tension stroke, the deceleration of the motor vehicle relative to the occupant thrusts the occupant forward against the seat belt, and the thrust is transferred to the shuttle through the connecting member. The shuttle is then propelled by the occupant's thrust in a direction opposite to the original tension direction, but immediately stopped by its self-locking mechanism, whose steel balls roll out from their neutral position to wedge between the inner surface of the tube and the conical portion of the shuttle to prevent it from reversing (see Fig. 2).

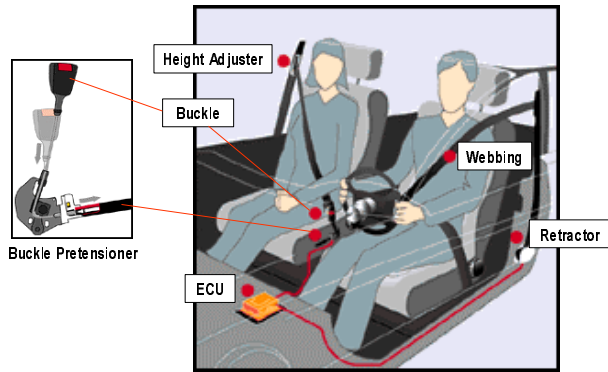


**Figure 1. A typical seat belt system with a linear buckle pretensioner.**

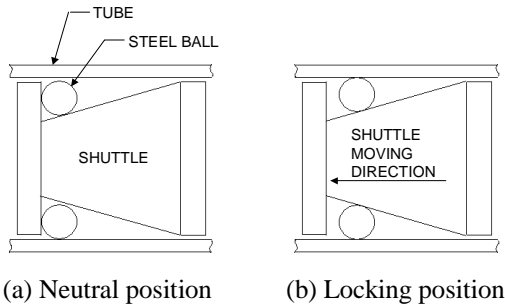


**Figure 2. The self-locking mechanism.**

However, after the pretensioner has accomplished its task, the crash event has just begun. The deceleration of the motor vehicle relative to the occupant further thrusts the occupant forward against the seat belt to yield the occupant restraint force. While this restraint force may be well below the injury threshold for many crash events, there are occasions when the occupant restraint force may exceed the injury threshold. One way to reduce this injury risk is to use a load-limiter to complement the pretensioner by regulating the maximum restraint force. An even better way is to re-utilize the pretensioner as a load-limiter by taking advantage of the displacement generated by the pretensioning operation. In this case, the additional packaging space, mass and cost associated with a load-limiter can be avoided.

The basic concept of the linear buckle pretensioner and load-limiter combo is very simple. Recall that the self-locking function of a buckle pretensioner is realized by allowing the steel balls to roll out from their neutral position to wedge between the inner surface of the tube and the conical portion of a shuttle. This suggests that the penetration depth of the balls into the tube wall could be used to control the level of the locking force. Accordingly, a gap between the inner surface of the tube and the outer surface of

the conical shuttle is introduced for controlling the penetration depth of the balls into the tube wall (see Fig. 3), which in turn, controls the locking force level to enable the reverse motion of the shuttle. The device now functions as a load-limiter, which can regulate the maximum belt webbing force within a desired limit. That is, at the conclusion of the pretensioning stroke, the device is essentially transformed from a pretensioner to a load-limiter due to the introduction of the gap [2]. Since the main difference is in the design details of its self-locking mechanism, the basic structural elements of such a device are almost identical to the original pretensioner (see Fig. 4).

Note that the modified locking mechanism is now essentially a rolling torus energy absorber [3], which is known for producing a rather consistent uniform resistance force throughout its energy absorption operation. This special characteristic is ideally suited for a load-limiter. An optimal resistance force can be chosen to ensure that the seat belt webbing force will be below the injury threshold of the thorax while the total amount of crash energy to be absorbed is maximized due to this uniform resistance force characteristic.

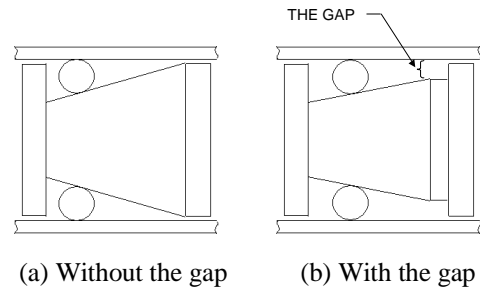


**Figure 3. Shuttle designs with and without the gap.**

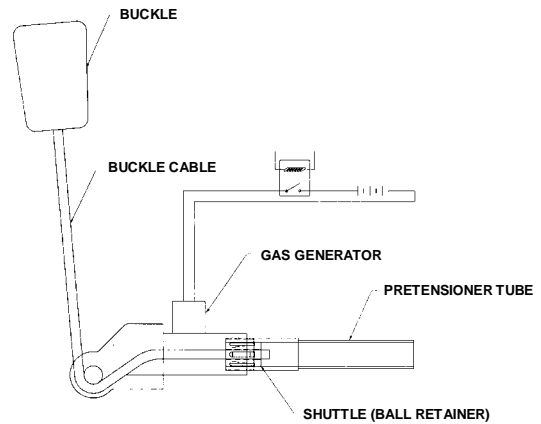


**Figure 4. Schematic diagram of the seat belt pretensioner and load-limiter combo [2].**

## PROTOTYPE AND TEST RESULTS

To demonstrate how the gap transformed a pretensioner to a load-limiter, a prototype device was designed, built and tested. In order to better control the plowing process of the rolling torus energy absorber, we use a cylindrical shape shuttle with slots to replace the conical portion of the shuttle. Each slot includes a wedge-shaped segment having a deep end, a shallow end and a flat segment. The flat segment merges with the wedge-shaped segment at the shallow end to introduce the desired gap. Steel balls are placed in the slots (no more than one per slot). The diameter of each of the steel balls is less than the depth of the wedge-shaped segment of the corresponding slot at the deep end and is greater than the depth of the flat segment of the corresponding slot. The tube was made of mild steel (AISI 1018), while a much harder material was used for the steel balls (ball bearing material) and shuttle (AISI 1030). Although the prototype device is capable of using up to six steel balls, only three steel balls are used here to demonstrate the concept. As expected, we observed that the only deformable part was the tube wall and that there were no permanent deformation on the steel balls and the guiding slots on the shuttle in the tests (see Fig. 5).

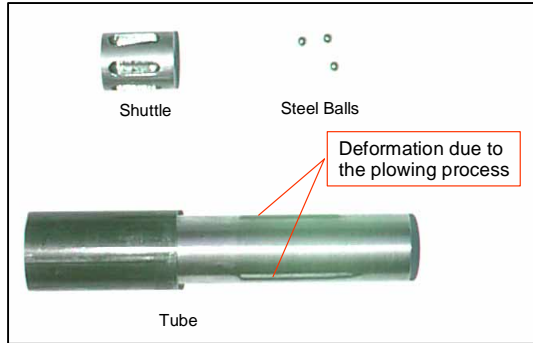


Figure 5. The the prototype after testing.

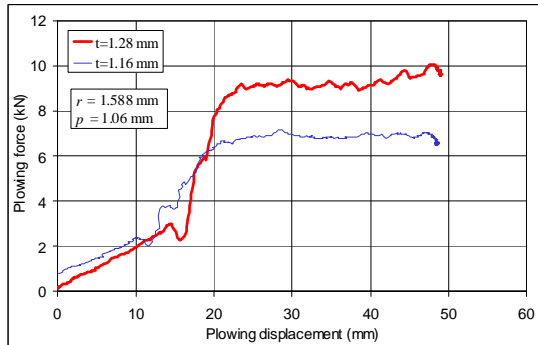


Figure 6. Test results.

Figure 6 depicts the plots of the measured force versus plowing displacement of two design variations. Observe that both curves consist of three distinctive stages: the rather linear beginning, the rapid jump, and finally, the plateau. The beginning stage characterizes the initial load increase due to the elastic deformation of the tube material. Once the penetration passes the yield point of the tube material, the second stage begins and quickly ends after the balls reached their full penetration depth. The final stage (i.e., the plateau) delivers the steady state plowing force, which is called the load-limiting force.

## PLOWING FORCE

A simple mechanics model (see Fig. 7) is developed for the linear pretensioner and load-limiter combo device to predict the plowing force and to understand relations among system variables including the tube wall thickness, ball diameter, penetration depth, tube material strength and friction coefficient. The approach is first to identify all primary deformation modes (i.e., energy absorbing modes) in the ball plowing process, and then calculate the energy dissipated in those modes. Finally, we find the plowing force through balance of internal work and external work.

As shown in the plowing model, the plowed groove is segmented into three regions: Region I is the leading spherical part and the ball is always underneath it during the plowing process; Region II is the middle cylindrical part which roughly covers the stable plowing distance; and Region III is the beginning part characterizing the penetration process associated with the initial load increase that occurs before reaching the full plowing force level. Since we are more interested in the stable plowing force, the beginning part (Region III) is not included in our analysis.

Balance of internal work and external work of all the balls gives the plowing force,  $F$ , we obtain

$$F = \frac{2n\sigma_0 t [t\theta + r(\theta - \sin \theta)]}{g(\theta, \mu)} \quad (1).$$

where  $n$  is the number of balls,  $\sigma_0$  is the yield stress of the tube material,  $t$  is the thickness of the outer tube wall,  $r$  is the common radius of the balls,  $\mu$  is the coefficient of friction between ball and tube, and

$$g(\theta, \mu) = 1 - \frac{1}{\cos \frac{\theta}{2} + \frac{1}{\mu} \sin \frac{\theta}{2}} \quad (2).$$

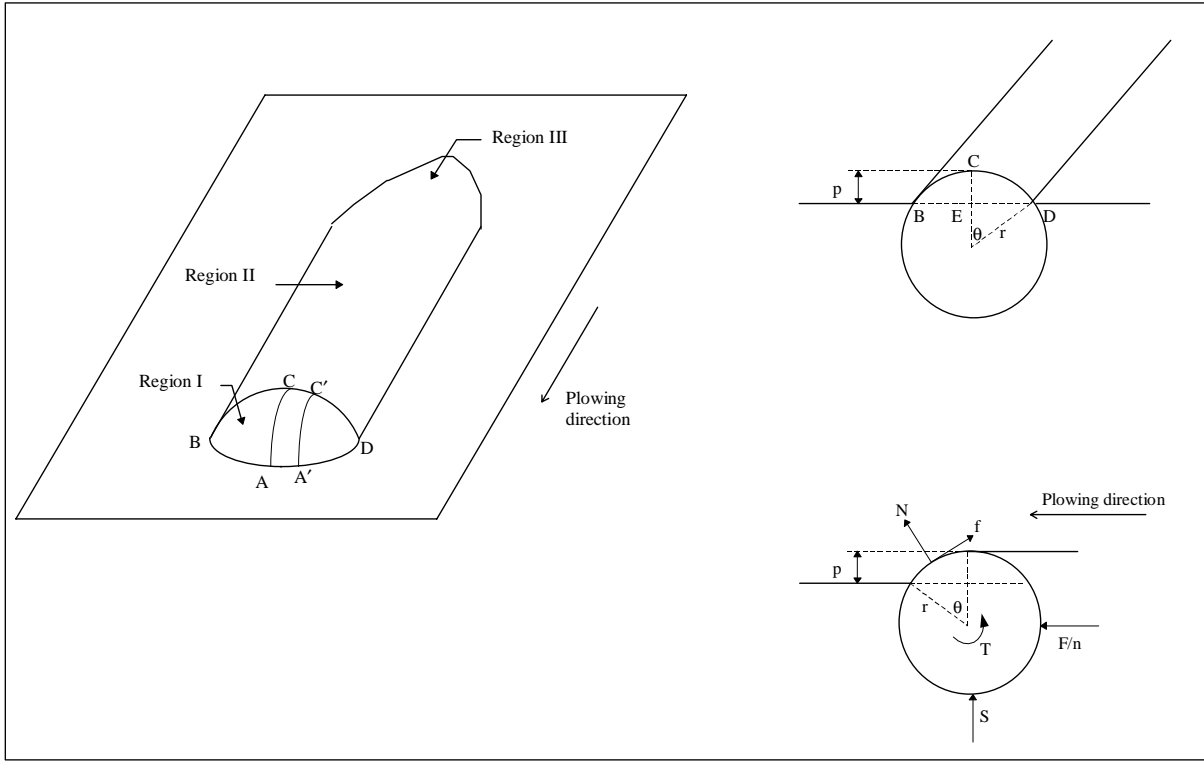


**Figure 7. The plowing model.**

## VALIDATION

We used hardware similar to the prototype described in Fig. 5 to verify the validity of the mathematical model of the plowing act. Four different tube wall thickness, 0.47, 0.52, 1.16 and 1.28 mm, are chosen for model verification. As will be shown they generally lead to the forces that cover the range of our interest (1 to 10 kN). Two material-related properties, the yield stress of the tube material and the friction coefficient  $\mu$  between tube wall and balls, are determined based on the ASM Metals Reference Book [4]. Based on data for 1015 steel and 1020 steel, the yield stress of the tube material (1018 steel) is in the range of 290 to 335 MPa and the ultimate tensile strength is in the range of 390 to 434 MPa, depending on heat treatment. Also, since the highest strain in plowing may reach strain-hardening level, a yield stress range of 300 to 350 MPa is used to account for the strain-hardening factor. The friction coefficient  $\mu$  may range from 0.2 to 0.4 and an average value, 0.3, is used to compare with the tests.

The plowing force versus the tube wall thickness predicted using Eq. (1) is plotted in Fig. 8 along with the test results. The other design parameters are: ball radius  $r=1.5875$  mm, penetration

$p=1.06$  mm and  $\theta$  is determined by the following geometric relationship:

$$\cos \theta = \frac{r - p}{r} = 1 - \frac{p}{r} \quad (3).$$

The four test points agree well with the parabolic relation between plowing force and tube wall thickness predicted by the analytical model.

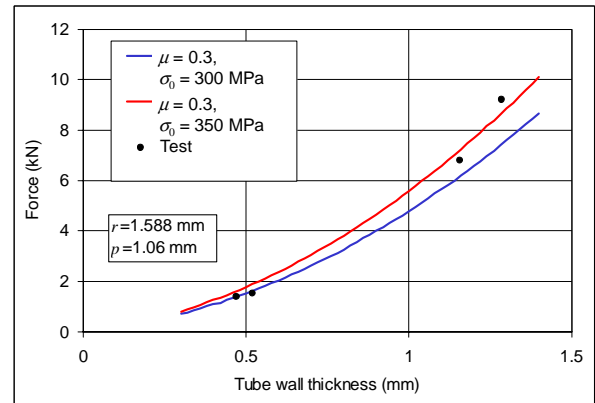


**Figure 8. Predicted and measured plowing forces vs. tube wall thickness.**

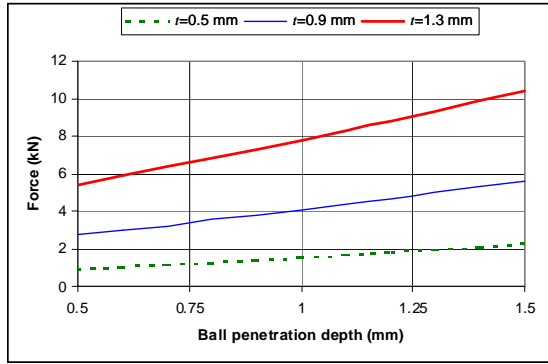


**Figure 9. Predicted plowing force vs. penetration depth.**

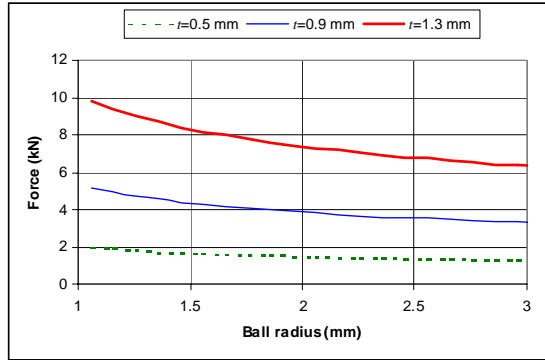


**Figure 10. Predicted plowing force vs. ball radius.**

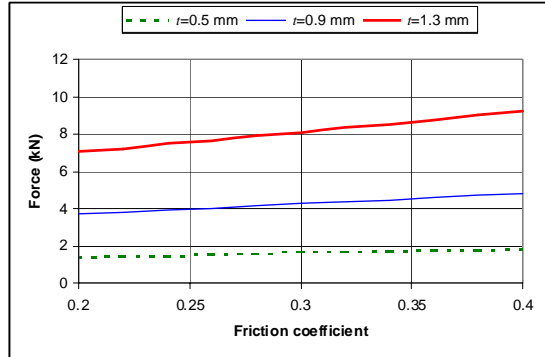


**Figure 11. Predicted plowing force vs. friction coefficient.**

## PARAMETER STUDY

We conducted a parameter study to demonstrate the dependence of plowing force on each design parameter. Three steel balls are used throughout this study. Since Eq. (1) suggests that the plowing force is a linear function of the yield stress of the tube material and the number of balls, we exclude them from our parameter study for obvious reason. The

tube wall thickness effect is also excluded from the parameter study, since the parabolic relation between plowing force and tube wall thickness is already displayed in Fig. 8. Three evenly distributed tube wall thickness, 0.5, 0.9 and 1.3 mm, and 320 MPa yield stress for the tube material are used in the parameter study. Results of the dependence of plowing force on the design parameters corresponding to the ball penetration depth, ball radius and friction coefficient about a reference design with  $p=1.06$  mm,  $r=1.5875$  mm, and  $\mu=0.3$ , are depicted in Figs. 9 through 11. The relations determined are useful for guiding the design of the linear pretensioner and load-limiter combo device.

## DESIGNS WITH EXTENDED STROKE

When a longer load-limiting stroke than the pretensioning stroke is desired, a tube section could be added to the other end of the gas generator [5]. For naming purposes, we refer to the added part as the lower tube and the original tube as the upper tube. Two designs, a break away reaction disc design (see Fig. 12) and a crushable foam insert design (see Fig. 13), are proposed here to reduce the initial volume of the space between the shuttle and the shuttle stop. With these two designs, the size of the gas generator can be reduced with a smaller initial volume to fill.

In a normal operation of the linear pretensioner and load-limiter combo with an extended load-limiting stroke, the shuttle is initially positioned near the gas generator end of the upper tube. When a severe crash event is detected by an onboard crash sensing system of the motor vehicle, an electrical signal will be sent to the gas generator to activate the gas generation process. The gas pressure will then push the shuttle toward the other end of the upper tube to perform the pretensioning operation. At the end of the pretensioning operation, the pull force from the seat belt webbing will force the shuttle to move in reverse. The slope of the slots on the shuttle will then act as a wedge to force steel balls to engage with the inner wall of the upper tube, and eventually the lower tube, to produce resistant force for the load-limiting operation. Notice that a portion of both upper and lower tubes, which is directly engaged with the housing of the gas generator, has a slightly larger inner diameter to maintain the desired resistance force under this increased tube wall thickness situation. The motion of the shuttle will then be halted after the webbing force becomes less than the resistant force of the plowing act or by a mechanical stop at the end of the lower tube.

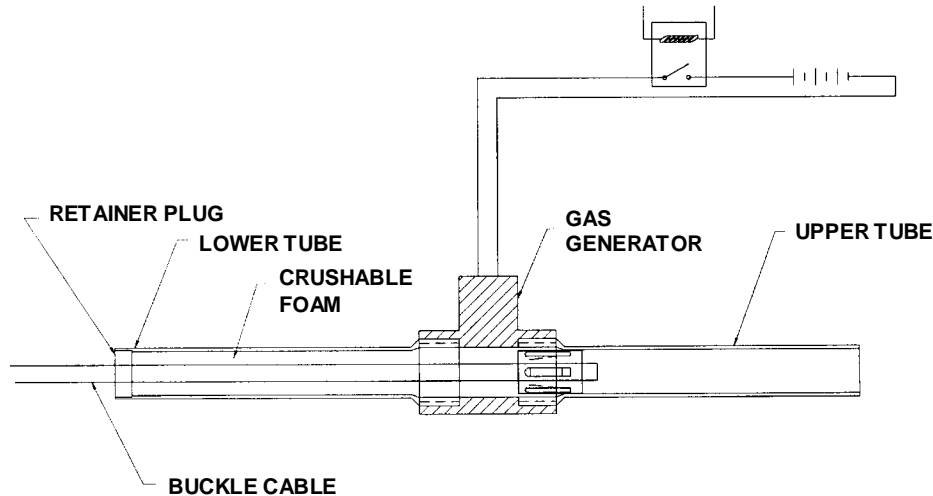


**Figure 12. An extended-stroke linear pretensioner and load-limiter combo with a breakaway reaction disc.**

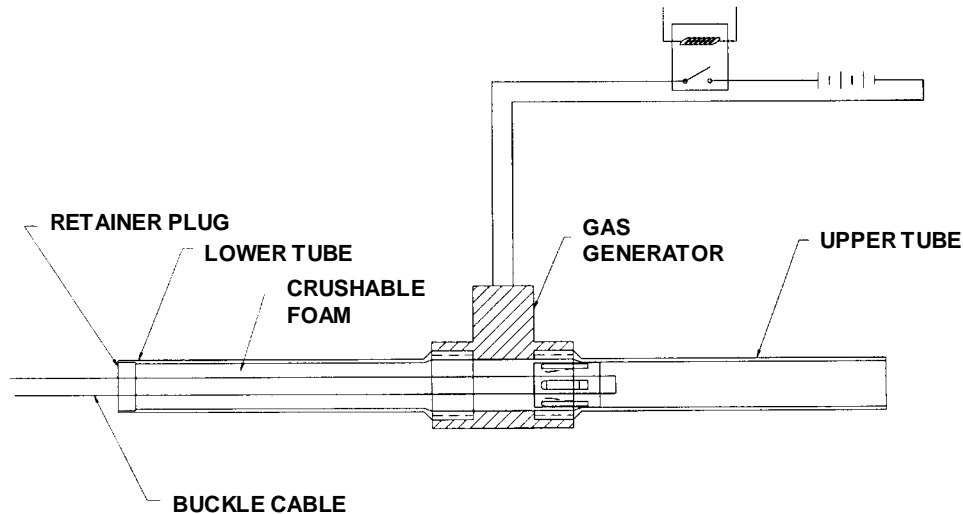


**Figure 13. An extended-stroke linear pretensioner and load-limiter combo with a crushable foam insert.**

## SUMMARY

A linear seat belt pretensioner and load-limiter combo device is presented. The basic structural elements of such a device are almost identical to a linear buckle pretensioner. It is realized by modifying the design of the self-locking mechanism of a buckle pretensioner. A small gap is introduced into the self-locking mechanism for controlling the locking force level through the penetration depth of its locking balls. The gap is so designed that it allows the locking balls, after the pretensioning operation, to plow through the tube material under a desired load and thus perform as a load-limiter. A prototype was designed and tested to demonstrate the concept. In this two-in-one design, the webbing displacement induced by the operation of a

linear buckle pretensioner is reused for load-limiting purposes. An advanced design with an extended load-limiting stroke is also presented. A mechanics model is developed to analytically estimate the load-limiting force and to understand relations among system variables and performance. Using this model, the equation for the load-limiting force is derived and verified with test data. This equation can be used to aid in the design of load-limiting devices. Since the combo device is only the size of a pretensioner, it eliminates the additional packaging requirement, as well as the mass and cost associated with an additional load-limiter. Due to its linear construction, the linear pretensioner and load limiter combo device can be integrated into the seat belt buckle and/or the shoulder belt height adjuster.

## ACKNOWLEDGMENT

The authors thank Mr. Edward Jedrzejczak for drafting design drawings and conducting tests. The authors also thank Drs. Bob Lust, Paul Meernik and Ching-Shan Cheng for reviewing the manuscript and for their comments.

## REFERENCES

1. Kock, Hans-Otto, 1999, "Seat Belt Systems: State of the Art and Future Trends," *ATZ Automobiltechnische Zeitschrift* 101 (1999)10.
2. Wang, J. T., 1994, "Seat Belt Pretensioner and Load-limiter," Research Disclosure No. 36852, Page 695.
3. Lin, K.-H. and Mase, G. T., 1990, "An Assessment of Add-on Energy Absorbing Devices for Vehicle Crashworthiness," *ASME Journal of Engineering Materials and Technology*, Vol. 112, pp. 406-411.
4. ASM Metals Reference Book, American Society for Metals, 2nd edition, p.211, 1983.
5. Wang, J. T., Zhou, Q., and Jedrzejczak, E., 2000, "Belt Tension and Energy Absorbing Apparatus," U.S. Patent No. 6,076,856.